Diet-induced Renal Changes in Zucker Rats Are Ameliorated by the Superoxide Dismutase Mimetic TEMPOL

Philip J. Ebenezer[1], **Nithya Mariappan**[1], **Carrie Elks**[1], **Masudul Haque**[1], and **Joseph Francis**[1]

[1] Department of Comparative Biomedical Sciences, LSU School of Veterinary Medicine, Louisiana State University, Baton Rouge, Louisiana, USA

Abstract

Diabetic nephropathy is the leading cause of renal failure in the United States. The obese Zucker rat (OZR; *fa/fa*) is a commonly used model of type 2 diabetes and metabolic syndrome (MetS), and of the nephropathy and renal oxidative stress commonly seen in these disorders. Heterozygous lean Zucker rats (LZRs; *fa/+*) are susceptible to high-fat diet (HFD)-induced obesity and MetS. The present study was designed to investigate whether superoxide scavenger 4-hydroxy-2,2,6,6-tetramethylpiperidinyloxy (TEMPOL), a membrane-permeable radical scavenger, could alleviate the renal effects of MetS in OZR and LZR fed a HFD, which resembles the typical "Western" diet. OZR and LZR were fed a HFD (OZR-HFD and LZR-HFD) or regular diet (OZR-RD and LZR-RD) and allowed free access to drinking water or water containing 1 mmol/l TEMPOL for 10 weeks. When compared to OZR-RD animals, OZR-HFD animals exhibited significantly higher levels of total renal cortical reactive oxygen species (ROS) production, plasma lipids, insulin, C-reactive protein, blood urea nitrogen (BUN), creatinine (Cr), and urinary albumin excretion ($P < 0.05$); these changes were accompanied by a significant decrease in plasma high-density lipoprotein levels ($P < 0.05$). The mRNA expression levels of desmin, tumor necrosis factor-α (TNF-α), nuclear factor κB (NFκB), and NAD(P)H oxidase-1 (NOX-1) were significantly higher in the renal cortical tissues of OZR-HFD animals; NFκB p65 DNA binding activity as determined by electrophoretic mobility shift assay was also significantly higher in these animals. The same trends were noted in LZR-HFD animals. Our data demonstrate that TEMPOL may prove beneficial in treating the early stages of the nephropathy often associated with MetS.

INTRODUCTION

Metabolic syndrome (MetS) consists of several inter-related metabolic risk factors, including dyslipidemia, hypertension, and hyperglycemia, and underlying factors such as obesity and insulin resistance, which give rise to the metabolic risk factors (1,2). The risk for developing comorbidities including type 2 diabetes mellitus, cardiovascular disease, and renal dysfunction increases dramatically as the number of components of MetS manifested in the patient increase (3). Further, diabetes mellitus is the leading cause of end-stage renal disease (i.e., kidney failure requiring transplantation or dialysis) in the United States, and affects over 40% of patients (4); this is because diabetic nephropathy occurs in 30–40% of diabetics (5). Thus, a thorough

understanding of the molecular mechanisms behind the renal dysfunction seen in MetS is paramount.

The MetS patient tends to have what is referred to as a "proinflammatory state," as demonstrated by elevations in acute phase reactants and proinflammatory cytokines (2,6), and increased systemic oxidative stress (7,8). Notably, four of the risk factors for MetS (dyslipidemia, hyperglycemia, obesity, and hypertension) are each independently characterized by increased oxidative stress and a proinflammatory state (3,6,7,9–14). An atherogenic diet (high in saturated fat and/or cholesterol), which resembles the typical "Western" diet (15,16), is also known to exacerbate oxidative stress and inflammation and contribute to MetS (2,14).

The obese Zucker rat (OZR) shares many characteristics with human MetS (such as insulin resistance, obesity, inflammation, and hyperlipidemia) and spontaneously develops nephropathy, and is therefore considered a model of MetS, type 2 diabetes mellitus, and diabetic nephropathy (17,18). OZR develop glomerular hypertrophy by ~3 months of age (19) and express albuminuria ~14 weeks of age (20); however, these animals do not exhibit glomerulosclerosis until 6–7 months of age (20,21). The OZR is also known to exhibit increased oxidative stress (22,23), which likely has a role in some of the renal injury seen in these animals (22,24).

Zucker rats carrying one copy of the *fa* allele (lean heterozygotes) are predisposed to diet-induced metabolic disturbances, including hyperinsulinemia and dyslipidemia, which contribute to the development of MetS (25,26). Because an atherogenic diet is known to perpetuate some components of MetS, we fed young OZR (*fa/fa*) and heterozygous lean Zucker rat (LZR) (*fa/+*) a high-fat diet (HFD) for 10 weeks, to induce oxidative stress and overt renal damage earlier in the life span, and assessed renal structural and functional parameters in these animals as compared to animals supplemented with the membrane-permeable free radical scavenger superoxide scavenger 4-hydroxy-2,2,6,6-tetramethylpiperidinyloxy (TEMPOL). We chose to use an atherogenic diet because it closely represents the typical "Western" diet. We chose to examine the effects of high-fat feeding on the kidney, as the kidney is largely responsible for blood pressure control and for some of the excess glucose release seen in the hyperglycemia of MetS and type 2 diabetes (27), as well as because nephropathy is the most common cause of end-stage renal disease in diabetic patients (4,5).

The actual quantitative effects of TEMPOL on reactive oxygen species (ROS) production in the renal cortical tissues of Zucker rats have not yet been examined; therefore, we used electron paramagnetic resonance spectroscopy to quantify changes in ROS production among groups. We also performed several quantitative measurements on glomeruli from all groups, to determine whether TEMPOL supplementation could attenuate the changes caused by a HFD and lead to improvements in renal function and renal redox status.

METHODS AND PROCEDURES

Experimental design

Five-week old heterozygous LZR (*fa/+*) and homozygous OZR (*fa/fa*), with initial body weights of ~120 g, were purchased from Harlan and housed in individual metabolic cages in a temperature- (23 ± 2 °C), humidity-, and light- (12-h light/dark cycle) controlled environment. Animals were fed either standard rodent chow (Rodent Diet 5001, with 14% fat-derived calories, 29% protein-derived calories, and 58% carbohydrate-derived calories; LabDiet, Richmond, IN) or HFD (modified AIN-93G, with 35% fat-derived calories, 15% protein-derived calories, and 50% carbohydrate-derived calories; Dyets, Bethlehem, PA), depending

on group assignments. More detailed information on each diet is included in **Supplementary Table S1** online.

Rats were divided into six groups (*n* = 8 each) as follows: group I: LZR-regular diet (LZR-RD), group II: LZR-HFD, group III: LZR-HFD-TEMPOL (LZR-HFD-TEM), group IV: OZR-RD, group V: OZR-HFD, group VI: OZR-HFD-TEMPOL (OZR-HFD-TEM). Groups I and IV were fed standard rodent chow and allowed free access to drinking water. Groups II and V were fed a HFD and allowed free access to drinking water. Groups III and VI were fed a HFD and allowed free access to water containing TEMPOL (1 mmol/l) for a total of 10 weeks. Food consumption and body weight were measured weekly. All experimental procedures were approved by the Louisiana State University Institutional Animal Care and Use Committee, and were performed in accordance with the National Institutes of Health Guide for the Care and Use of Laboratory Animals.

Blood pressure measurements

Tail systolic and mean arterial blood pressures were measured as previously reported (28,29).

Nonfasting blood, plasma, and urine analyses

Blood glucose was estimated with an Ascensia Elite glucometer according to the manufacturer's instructions (Bayer, Elkhart, IN). Plasma insulin levels were measured using an ultrasensitive rat insulin enzyme-linked immunosorbent assay kit (Crystal Chem, Downers Grove, IL) according to the manufacturer's instructions. Urine albumin concentration was determined using a Nephrat II Albumin kit (Exocell, Philadelphia, PA).

Blood urea nitrogen (BUN), creatinine (Cr), and BUN/Cr in plasma were determined using a Stat Profile Critical Care Xpress Analyzer (Nova Biomedical) according to the manufacturer's instructions. C-reactive protein was measured in plasma by a kit method (Alpco Diagnostics, Salem, NH) according to the manufacturer's protocol. Levels of total cholesterol, high-density lipoprotein and low-density lipoprotein/very low-density lipoprotein in plasma were quantified by a kit method (Biovision, CA) as per the manufacturer's instructions.

Measurement of total ROS

Total ROS in the kidney cortex was measured by electron paramagnetic resonance spectroscopy as described earlier (29).

Histology

For histological evaluations using light microscopy, longitudinal sections of one kidney from each animal were fixed in 10% buffered formalin, embedded in parafin, cut into 2 μm-thick sections, and then stained with hematoxylin and eosin stain. Slides were then examined at ×20 magnification and measurements of glomeruli and mesangial area and perimeter were performed. A total of 40 glomeruli per section were randomly selected and measured by an observer blinded to the phenotype and treatment of each rat.

Transmission electron microscopy

Transmission electron microscopy studies were carried out as previously described (30).

Lucigenin assay

Lucigenin-enhanced chemiluminescence was used to measure NAD(P) H-dependent superoxide production in kidney cortex (29,31).

Immunofluorescence detection of desmin

Immunofluorescence studies were carried out as described earlier (29,32).

Gene expression profiles

Gene expression levels for desmin, tumor necrosis factor-α (TNF-α), nuclear factor κB (NFκB), and NAD(P)H oxidase-1 (NOX-1) were assessed by real-time reverse transcriptase-PCR as described earlier (28–30). Primers used appear in **Supplementary Table S2** online.

Electrophoretic mobility shift assay

Electrophoretic mobility shift assay was performed as described earlier (29,33).

Statistical analysis

Statistical analyses were performed using one-way ANOVA with repeated measurements. Post hoc Bonferroni procedures were used for comparisons of treatment groups. For lucigenin assay, a two-way repeated measures ANOVA was used. $P < 0.05$ was considered statistically significant. Values are expressed as means ± s.e.m.

RESULTS

Effect of TEMPOL on blood pressure and metabolic parameters

As expected, the systolic and mean arterial blood pressures of OZR-HFD animals were significantly higher than those of OZR-RD and OZR-HFD-TEM animals (Table 1). No changes in systolic or mean arterial blood pressure were noted among any of the LZR. OZR-HFD animals also had significantly higher body weights and average weight gain than other OZR, with a similar trend observed in LZR. OZR-RD animals consumed a significantly higher quantity of food than all other OZR. TEMPOL treatment had no effect on food intake in LZR. OZR animals fed a HFD exhibited significant increases in liver, kidney, and abdominal fat pad weight (Table 1).

Effect of TEMPOL on plasma chemistries and plasma lipids

Plasma Cr, BUN, urine albumin excretion, and C-reactive protein (an inflammatory marker) were all significantly higher in OZR-HFD animals than in OZR-RD animals; TEMPOL normalized these parameters in OZR (Table 2). LZR-HFD animals also had increased plasma C-reactive protein levels when compared to LZR-RD animals, and TEMPOL treatment significantly attenuated this increase.

Plasma glucose and insulin levels were significantly higher in OZR-HFD animals when compared with OZR-RD animals. LZR-HFD animals also demonstrated increased plasma glucose and insulin levels when compared to LZR-RD animals. TEMPOL treatment significantly attenuated this increase in OZR and LZR.

Total cholesterol, very low-density lipoprotein cholesterol, and triglycerides were significantly higher in OZR-HFD animals than OZR-RD animals, with a similar trend observed in LZR animals (Table 3). High-density lipoprotein levels were significantly lower in the OZR-HFD group when compared to the OZR-RD group, with the same trend observed in the LZR groups. TEMPOL restored high-density lipoprotein to near control levels in both OZR and LZR animals (Table 3).

Total cortical ROS production

Actual spectra from electron paramagnetic resonance experiments appear in Figure 1a, along with results in graphical form. A significant increase in total ROS production was observed in

renal cortical tissues of OZR-HFD animals when compared with those of OZR-RD animals; the same trend was noted in LZR. TEMPOL attenuated these increases in cortical ROS production.

Lucigenin assay

OZR-HFD animals had higher levels of superoxide production than OZR-RD animals. The same trend was observed in LZR animals. Overall cortical superoxide production was lower in LZR than in OZR. In both OZR-HFD and LZR-HFD animals, TEMPOL treatment significantly reduced superoxide production. Results are presented graphically in Figure 1b.

Glomerular histology

Glomerular diameter, area, and circumference were all significantly greater in the OZR-HFD animals than in any other group (Table 4). When compared to LZR-RD animals, LZR-HFD animals exhibited significant decreases in glomerular diameter, area, and circumference. TEMPOL treatment attenuated these changes (Table 4).

Podocyte morphology and glomerular ultrastructure

Podocyte morphology and glomerular ultrastructure were normal in both the LZR-RD groups (Figure 2a) and OZR-RD (Figure 2e). In OZR-HFD animals, podocyte injury was observed (Figure 2f). TEMPOL treatment normalized podocyte morphology in OZR-HFD animals (Figure 2h). The degree of podocyte damage was compared with the degree of fluorescence observed in the kidney cortex sections by using desmin (podocyte injury marker). Immunofluorescence studies show that desmin expression is absent in LZR-RD (Figure 3a) and OZR-RD (Figure 3b). LZR-HFD (Figure 4e) animals showed slight increase in the expression of desmin when compared with LZR-RD or OZR-RD. In contrast, the OZR-HFD animals showed a significant expression of desmin in the glomeruli (Figure 3f). Treatment with TEMPOL significantly attenuated desmin expression both in LZR as well as OZR fed with a HFD (Figure 3i,j).

Gene expression profiles

In OZR-HFD animals, increases in expression of desmin, TNF-α, NFκB, and NOX-1 were seen in the kidney cortex (Figure 4a); TEMPOL treatment significantly attenuated the increased expression of these genes. No statistically detectable changes were observed in the mRNA expression in LZR.

Electrophoretic mobility shifting assay

NFκB p65 DNA binding activity was analyzed in renal cortical nuclear extracts with electrophoretic mobility shift assay (Figure 4b). Densitometry analysis revealed significantly higher NFκB p65 DNA binding activity in OZR-HFD animals than in OZR-RD animals. The same trend was noted with LZR. TEMPOL attenuated the increases in NFκB p65 DNA binding activity.

DISCUSSION

A more thorough understanding of the mechanisms underlying the nephropathies seen in MetS and type 2 diabetes mellitus will allow more patients with this disease to be treated before end-stage renal disease ensues. We fed LZR and OZR a HFD, which closely resembles the typical "Western" diet, to accelerate the progression of overt renal disease in MetS. Results from our study demonstrate that HFD induces damage to the renal cortex by increasing oxidative stress and inflammation, and that the free radical scavenger, TEMPOL, ameliorates these alterations.

Our data suggest that the glomerular injury seen in MetS is driven by oxidative stress. Increased circulating glucose levels are known to increase oxidative stress by inducing excess production of mitochondrial ROS, which in turn activates other chemical pathways that produce additional ROS (34). Further, the tissue renin-angiotensin system is upregulated in MetS; thus, increased renal angiotensin may induce ROS production by NAD(P)H oxidases (35). It is likely that the overproduction of free radicals triggered excess free fatty acids in OZR-HFD and led to enhanced production of conjugated dienes and lipid hydroperoxides (36), thereby contributing to glomerular damage. The superoxide scavenging ability of TEMPOL caused significant decreases in plasma lipids; these changes may be partly responsible for the improved histological parameters we observed in the OZR-HFD-TEM group.

Interestingly, when LZR were fed a HFD, the resulting phenotype was quite similar to that of OZR. This suggests that, in the presence of an external stimulus such as an atherogenic diet, a single copy of the *fa* allele is sufficient to result in diet-induced obesity and its associated sequelae; these results support those of earlier studies conducted in heterozygous LZR (26, 37). In the presence of a RD, the only appreciable differences in metabolic parameters between LZR and OZR were in plasma insulin and urinary albumin excretion. This can likely be explained by the younger ages of the animals. At age 15 weeks, OZR fed a RD exhibit hyperfiltration, which is a renal compensatory mechanism (20); this compensation allows for maintenance of normal urine output, normal plasma Cr, and normal BUN. Glomerulosclerosis and chronic renal disease are generally not seen in these animals until ~6 months of age (20, 21). This theory is further supported by our morphological findings in the glomeruli of these animals. Glomerular area, glomerular diameter, and glomerular circumference all increased in OZR-RD when compared to LZR-RD, but these increases were not significant. However, increases of these measurements are consistent with the parameters expected in hyperfiltration. OZR-HFD animals exhibited glomerulomegaly and concomitant decreases in renal function, indicating that HFD had exacerbated the renal injury in these animals.

One of the early signs of nephropathy in Zucker rats is enhanced urinary albumin excretion (30). In this study, the OZR-RD and OZR-HFD groups showed significant increases in urinary albumin excretion. Microalbuminuria is connected with endothelial dysfunction, inflammation, and free radical generation (34). In this study, we observed increased urinary albumin excretion, along with increases in other inflammatory markers, which were associated with overproduction of total ROS and superoxide (Figure 1a) in OZR-HFD animals. The free radicals associated with inflammatory conditions are thought to contribute to MetS and insulin resistance (35), and are likely a major cause of the increased inflammation seen in the HFD-fed animals. It is well-known that proinflammatory cytokines increase superoxide production, which in turn increases NFκB, thereby leading to another cycle of increased proinflammatory cytokines and oxidative stress, thus amplifying the signal and resulting in end organ damage. This vicious cycle makes it difficult to determine whether the oxidative stress or increased NFκB activity comes first in our study; more in-depth studies are needed to elucidate the exact cause of our results.

Our electrophoretic mobility shift assay results demonstrate a significant increase in NFκB activity in kidney cortices of OZR-HFD animals (Figure 4b). These results were further supported with the increases in gene expression of desmin, TNF-α, NFκB, and NOX-1; total ROS estimation; and superoxide production (Figures 1a,b and 4a–d). We also saw differences in gene expression of desmin, TNF-α, NFκB, and NOX-1 between LZR-HFD and OZR-HFD animals, despite their having similar levels of oxidative stress. It is likely that this is because the OZR develops a basal level of oxidative stress at a very early age, whereas in the *fa/+* LZR, oxidative stress will only develop in the presence of an external stimulus. Therefore, the OZR has higher oxidative stress at baseline. Thus, even though overall levels of oxidative stress are similar, the ending message levels of proinflammatory genes may differ.

We assessed the extent of renal inflammation present by immunofluorescence staining of desmin. Desmin is an intermediate filament protein (36,38) and a podocyte damage marker, which is present in glomerular mesangial cells and is highly expressed in podocytes, exclusively in the setting of glomerular injury (37). Podocyte damage was assessed by using immunofluorescence and transmission electron microscopy studies. The expression of desmin at the glomerular edge rapidly progressed in OZR-HFD animals, which is likely a result of the marked increases in inflammation and ROS production. Increased desmin expression in glomeruli injured by intraglomerular hypertension, hyperlipidemia, monocyte/macrophage glomerular infiltration, and glomerular hypertrophy has been well established by earlier research (3,33,38). Interestingly, podocyte foot processes and the remaining glomerular ultrastructure, particularly mesangial cells, were well-preserved in LZR-HFD-TEM- and OZR-HFD-TEM-animals (Figure 2d,h).

Although our results suggest that a HFD can exacerbate the nephropathy seen in MetS, they must be interpreted with some caution, as limitations to this study do exist. First, the known blood pressure–lowering effects of TEMPOL could be responsible for the beneficial effects of this drug on renal parameters of MetS in our animals; thus, in our ongoing studies, we are using drugs with combined antioxidant and hypotensive effects, and drugs without hypotensive or antioxidant effects. These studies should allow us to separate the blood pressure effects from the antioxidant effects seen in the present study. Second, we compared a semipurified experimental HFD with a standard, nonpurified chow control. Many other groups have conducted similar studies with similar diets (addressed in ref. 39) and did not see any appreciable alterations in their results; however, the "ideal" HFD has not yet been defined. Thus, it is possible that the types of fats as well as the increased energy value of the HFD (**Supplementary Table S1** online) we used may have affected our results.

In conclusion, in young OZR and LZR fed a HFD, treatment with the membrane-permeable SOD mimetic TEMPOL for 10 weeks induces significant improvements in blood pressure, ROS production, and renal cortical structure and function. Future studies should focus on the exact sources of ROS that contribute to these abnormalities in this animal model of MetS.

Acknowledgments

References

1. Reaven GM. Banting lecture 1988. Role of insulin resistance in human disease. Diabetes 1988;37:1595–1607. [PubMed: 3056758]

2. Grundy SM, Cleeman JI, Daniels SR, et al. Diagnosis and management of the metabolic syndrome: an American Heart Association/National Heart, Lung, and Blood Institute Scientific Statement. Circulation 2005;112:2735–2752. [PubMed: 16157765]

3. Mundy AL, Haas E, Bhattacharya I, et al. Fat intake modifies vascular responsiveness and receptor expression of vasoconstrictors: implications for diet-induced obesity. Cardiovasc Res 2007;73:368–375. [PubMed: 17166491]

4. Friedman EA, Friedman AL. Is there really good news about pandemic diabetic nephropathy? Nephrol Dial Transplant 2007;22:681–683. [PubMed: 17205960]

5. Schena FP, Gesualdo L. Pathogenetic mechanisms of diabetic nephropathy. J Am Soc Nephrol 2005;16 (Suppl 1):S30–S33. [PubMed: 15938030]

6. Ridker PM, Wilson PW, Grundy SM. Should C-reactive protein be added to metabolic syndrome and to assessment of global cardiovascular risk? Circulation 2004;109:2818–2825. [PubMed: 15197153]

7. Fortuño A, San José G, Moreno MU, et al. Phagocytic NADPH oxidase overactivity underlies oxidative stress in metabolic syndrome. Diabetes 2006;55:209–215. [PubMed: 16380495]

8. Hansel B, Giral P, Nobecourt E, et al. Metabolic syndrome is associated with elevated oxidative stress and dysfunctional dense high-density lipoprotein particles displaying impaired antioxidative activity. J Clin Endocrinol Metab 2004;89:4963–4971. [PubMed: 15472192]

9. Bae JH, Bassenge E, Kim KB, et al. Postprandial hypertriglyceridemia impairs endothelial function by enhanced oxidant stress. Atherosclerosis 2001;155:517–523. [PubMed: 11254924]

10. Ceriello A. Possible role of oxidative stress in the pathogenesis of hypertension. Diabetes Care 2008;31(Suppl 2):S181–S184. [PubMed: 18227482]

11. Giugliano D, Ceriello A, Esposito K. The effects of diet on inflammation: emphasis on the metabolic syndrome. J Am Coll Cardiol 2006;48:677–685. [PubMed: 16904534]

12. Keaney JF Jr, Larson MG, Vasan RS, et al. Obesity and systemic oxidative stress: clinical correlates of oxidative stress in the Framingham Study. Arterioscler Thromb Vasc Biol 2003;23:434–439. [PubMed: 12615693]

13. Picchi A, Gao X, Belmadani S, et al. Tumor necrosis factor-alpha induces endothelial dysfunction in the prediabetic metabolic syndrome. Circ Res 2006;99:69–77. [PubMed: 16741160]

14. Riccardi G, Giacco R, Rivellese AA. Dietary fat, insulin sensitivity and the metabolic syndrome. Clin Nutr 2004;23:447–456. [PubMed: 15297079]

15. Kris-Etherton P, Eckel RH, Howard BV, St Jeor S, Bazzarre TL. AHA Science Advisory: Lyon Diet Heart Study. Benefits of a Mediterranean-style, National Cholesterol Education Program/American Heart Association Step I Dietary Pattern on Cardiovascular Disease. Circulation 2001;103:1823–1825. [PubMed: 11282918]

16. Mansouri RM, Baugé E, Gervois P, et al. Atheroprotective effect of human apolipoprotein A5 in a mouse model of mixed dyslipidemia. Circ Res 2008;103:450–453. [PubMed: 18658049]

17. Coimbra TM, Janssen U, Gröne HJ, et al. Early events leading to renal injury in obese Zucker (fatty) rats with type II diabetes. Kidney Int 2000;57:167–182. [PubMed: 10620198]

18. Gassler N, Elger M, Kränzlin B, et al. Podocyte injury underlies the progression of focal segmental glomerulosclerosis in the fa/fa Zucker rat. Kidney Int 2001;60:106–116. [PubMed: 11422742]

19. Lavaud S, Michel O, Sassy-Prigent C, et al. Early influx of glomerular macrophages precedes glomerulosclerosis in the obese Zucker rat model. J Am Soc Nephrol 1996;7:2604–2615. [PubMed: 8989739]

20. Kasiske BL, Cleary MP, O'Donnell MP, Keane WF. Effects of genetic obesity on renal structure and function in the Zucker rat. J Lab Clin Med 1985;106:598–604. [PubMed: 4056570]

21. Danis RP, Yang Y. Microvascular retinopathy in the Zucker diabetic fatty rat. Invest Ophthalmol Vis Sci 1993;34:2367–2371. [PubMed: 8505219]

22. Banday AA, Marwaha A, Tallam LS, Lokhandwala MF. Tempol reduces oxidative stress, improves insulin sensitivity, decreases renal dopamine D1 receptor hyperphosphorylation, and restores D1 receptor-G-protein coupling and function in obese Zucker rats. Diabetes 2005;54:2219–2226. [PubMed: 15983225]

23. Russo I, Del Mese P, Doronzo G, et al. Resistance to the nitric oxide/cyclic guanosine 5′-monophosphate/protein kinase G pathway in vascular smooth muscle cells from the obese Zucker rat, a classical animal model of insulin resistance: role of oxidative stress. Endocrinology 2008;149:1480–1489. [PubMed: 18079207]

24. Chander PN, Gealekman O, Brodsky SV, et al. Nephropathy in Zucker diabetic fat rat is associated with oxidative and nitrosative stress: prevention by chronic therapy with a peroxynitrite scavenger ebselen. J Am Soc Nephrol 2004;15:2391–2403. [PubMed: 15339988]

25. Corsetti JP, Sparks JD, Peterson RG, Smith RL, Sparks CE. Effect of dietary fat on the development of non-insulin dependent diabetes mellitus in obese Zucker diabetic fatty male and female rats. Atherosclerosis 2000;148:231–241. [PubMed: 10657558]

26. Henriksen EJ, Teachey MK, Lindborg KA, Diehl CJ, Beneze AN. The high-fat-fed lean Zucker rat: a spontaneous isocaloric model of fat-induced insulin resistance associated with muscle GSK-3 overactivity. Am J Physiol Regul Integr Comp Physiol 2008;294:R1813–R1821. [PubMed: 18385470]

27. Meyer C, Woerle HJ, Dostou JM, Welle SL, Gerich JE. Abnormal renal, hepatic, and muscle glucose metabolism following glucose ingestion in type 2 diabetes. Am J Physiol Endocrinol Metab 2004;287:E1049–E1056. [PubMed: 15304374]

28. Guggilam A, Haque M, Kerut EK, et al. TNF-alpha blockade decreases oxidative stress in the paraventricular nucleus and attenuates sympathoexcitation in heart failure rats. Am J Physiol Heart Circ Physiol 2007;293:H599–H609. [PubMed: 17416605]

29. Elks CM, Mariappan N, Haque M, et al. Chronic NF-{kappa}B blockade reduces cytosolic and mitochondrial oxidative stress and attenuates renal injury and hypertension in SHR. Am J Physiol Renal Physiol 2009;296:F298–F305. [PubMed: 19073636]

30. Mariappan N, Soorappan RN, Haque M, Sriramula S, Francis J. TNF-alpha-induced mitochondrial oxidative stress and cardiac dysfunction: restoration by superoxide dismutase mimetic Tempol. Am J Physiol Heart Circ Physiol 2007;293:H2726–H2737. [PubMed: 17675574]

31. Li YL, Gao L, Zucker IH, Schultz HD. NADPH oxidase-derived superoxide anion mediates angiotensin II-enhanced carotid body chemoreceptor sensitivity in heart failure rabbits. Cardiovasc Res 2007;75:546–554. [PubMed: 17499230]

32. Khaleduzzaman M, Francis J, Corbin ME, et al. Infection of cardiomyocytes and induction of left ventricle dysfunction by neurovirulent polytropic murine retrovirus. J Virol 2007;81:12307–12315. [PubMed: 17855522]

33. Liu D, Gao L, Roy SK, Cornish KG, Zucker IH. Neuronal angiotensin II type 1 receptor upregulation in heart failure: activation of activator protein 1 and Jun N-terminal kinase. Circ Res 2006;99:1004–1011. [PubMed: 17008603]

34. Nishikawa T, Edelstein D, Du XL, et al. Normalizing mitochondrial superoxide production blocks three pathways of hyperglycaemic damage. Nature 2000;404:787–790. [PubMed: 10783895]

35. Coughlan MT, Thallas-Bonke V, Pete J, et al. Combination therapy with the advanced glycation end product cross-link breaker, alagebrium, and angiotensin converting enzyme inhibitors in diabetes: synergy or redundancy? Endocrinology 2007;148:886–895. [PubMed: 17110423]

36. Inoguchi T, Li P, Umeda F, et al. High glucose level and free fatty acid stimulate reactive oxygen species production through protein kinase C--dependent activation of NAD(P)H oxidase in cultured vascular cells. Diabetes 2000;49:1939–1945. [PubMed: 11078463]

37. Maher MA, Banz WJ, Zemel MB. Variations of blood pressures in lean Zucker rats fed low or high fat diets. J Nutr 1995;125:2618–2622. [PubMed: 7562098]

38. Riley SG, Steadman R, Williams JD, Floege J, Phillips AO. Augmentation of kidney injury by basic fibroblast growth factor or platelet-derived growth factor does not induce progressive diabetic nephropathy in the Goto Kakizaki model of non-insulin-dependent diabetes. J Lab Clin Med 1999;134:304–312. [PubMed: 10482316]

39. Buettner R, Schölmerich J, Bollheimer LC. High-fat diets: modeling the metabolic disorders of human obesity in rodents. Obesity (Silver Spring) 2007;15:798–808. [PubMed: 17426312]
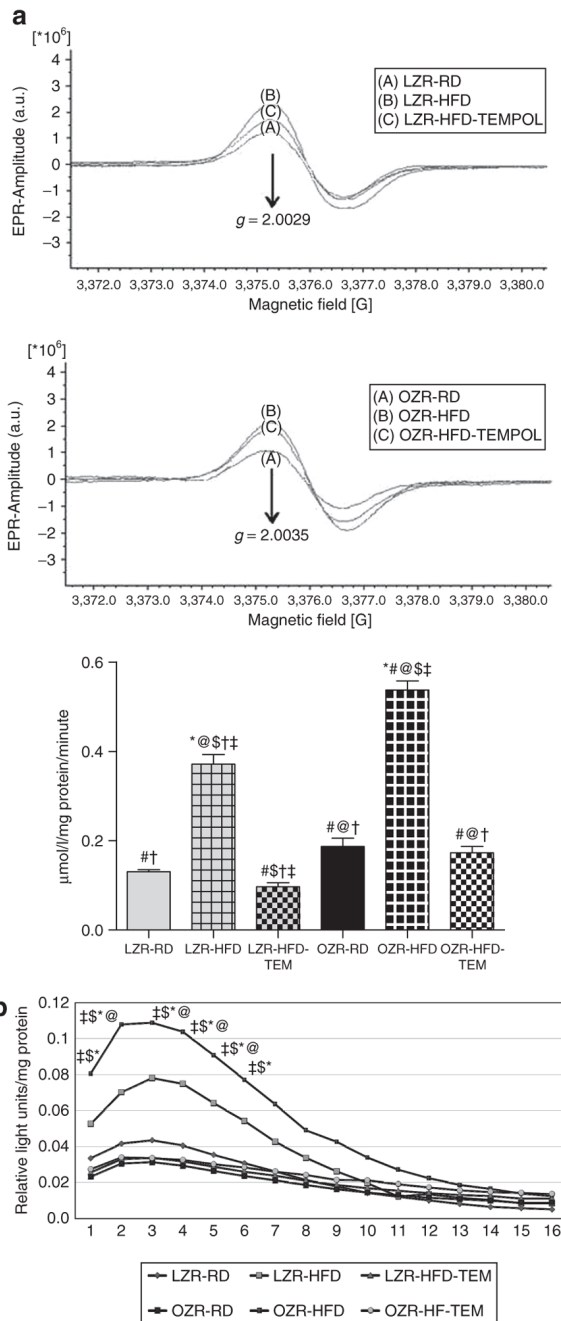
Figure 1.
(**a**) Total reactive oxygen species (ROS) production rates in renal cortical tissues from 15-week-old experimental animals as measured by electron paramagnetic resonance (EPR) spectroscopy. Values are expressed as means ± s.e.m. High-fat diet (HFD) significantly increased total ROS production in cortical tissues from both LZR and OZR; these increases were attenuated by TEMPOL treatment. (**b**) NAD(P) H-dependent superoxide production in homogenates of renal cortical tissues from 15-week-old experimental animals as measured by lucigenin assay. Values are expressed as means ± s.e.m., and are reported as relative light units/milligram protein. HFD significantly increased NAD(P) H-dependent superoxide production in both LZR and OZR; TEMPOL attenuated these increases. $^*P < 0.05$ vs. LZR-RD, $^#P < 0.05$

vs. LZR-HFD, $^{@}P < 0.05$ vs. LZR-HFD-TEM, $^{\$}P < 0.05$ vs. OZR-RD, $^{\dagger}P < 0.05$ vs. OZR-HFD, $^{\ddagger}P < 0.05$ vs. OZR-HFD-TEM. a.u., arbitrary unit; LZR, lean Zucker rat; OZR, obese Zucker rat; RD, regular diet; TEMPOL, superoxide scavenger 4-hydroxy-2,2,6,6-tetramethylpiperidinyloxy.
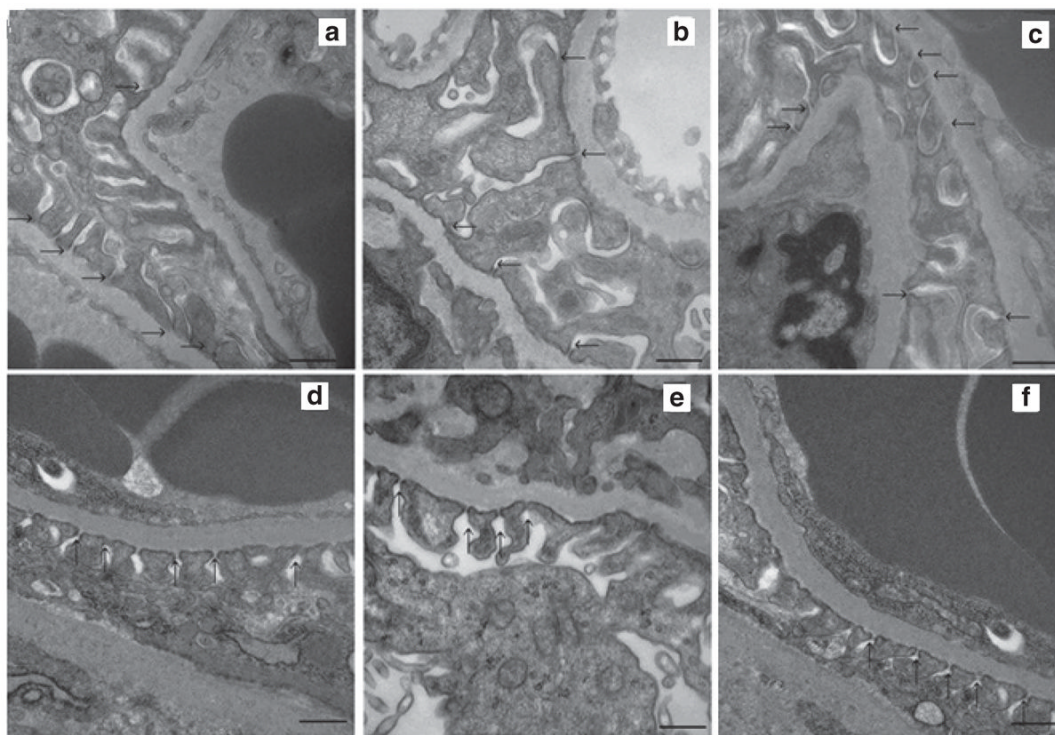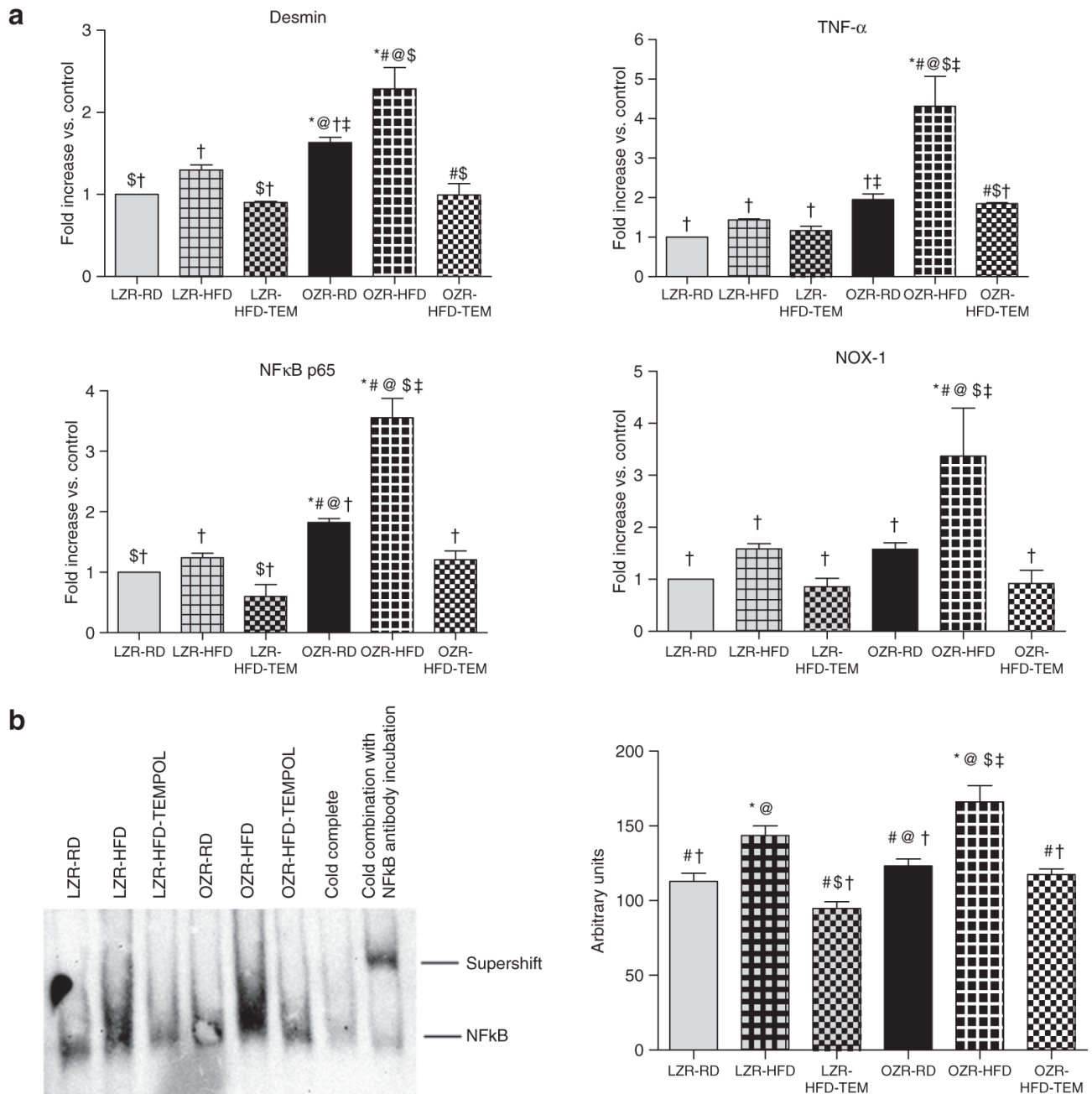
Figure 2.
Glomeruli of 15-week-old experimental animals as examined by transmission electron microscopy (×40,000 magnification; bar = 500nm). (**a**) Normal podocyte ultrastructure, with ordered and upright foot processes, in LZR-RD animals; (**b**) LZR-HF animals exhibited minimal podocyte damage, and (**c**) LZR-HFD-TEMPOL animals exhibited almost normal podocyte architecture. (**d**) Normal podocyte ultrastructure was observed in OZR-RD animals. (**e**) OZR-HFD animals exhibited fusion and shortening of foot processes, variation of the width of filtration slits, broadening of foot processes, fewer filtration slits per unit length, and multiple inclusion cysts or vacuoles within the cytoplasm of the podocytes. (**f**) OZR-HFD-TEMPOL animals exhibited almost normal podocyte ultrastructure. HFD, high-fat diet; LZR, lean Zucker rat; OZR, obese Zucker rat; RD, regular diet; TEMPOL, superoxide scavenger 4-hydroxy-2,2,6,6-tetramethylpiperidinyloxy.
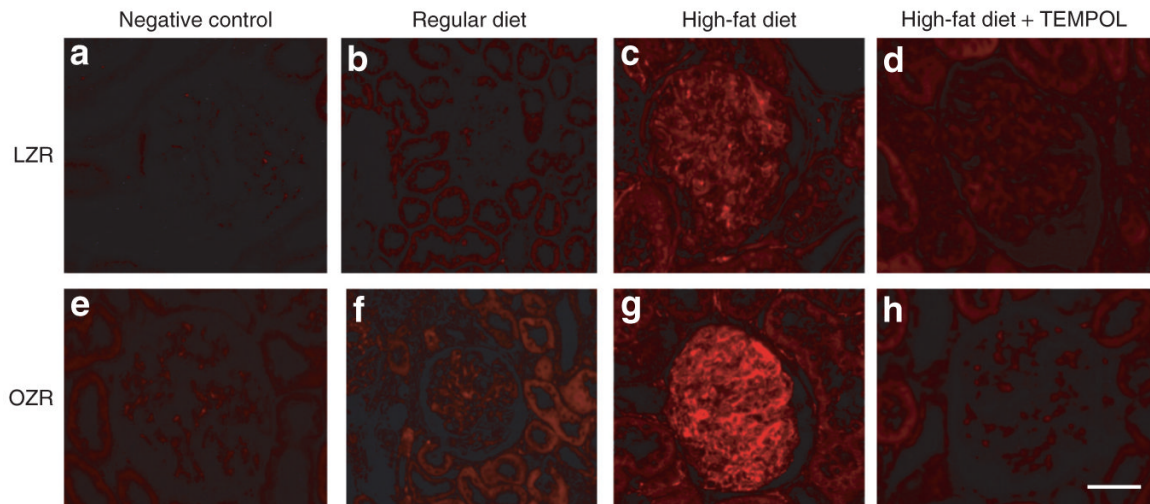
Figure 3.
(**a**) Immunofluorescent micrographs (×20 original magnification) of glomeruli of 15-week-old experimental animals stained for desmin. Negative controls are depicted in **a** and **e**. (**b**) LZR-RD glomeruli exhibited no detectable desmin expression; (**f**) few desmin positive cells were found in OZR-RD glomeruli; (**c**) LZR-HFD glomeruli exhibited increased expression of desmin; (**g**) OZR-HFD glomeruli exhibited a marked increase in desmin expression; (**d**) and (**h**) TEMPOL treatment attenuated desmin expression in both LZR-HFD-TEMPOL and OZR-HFD-TEMPOL animals. HFD, high-fat diet; LZR, lean Zucker rat; OZR, obese Zucker rat; RD, regular diet; TEMPOL, superoxide scavenger 4-hydroxy-2,2,6,6-tetramethylpiperidinyloxy.

Figure 4.
(**a**) Gene expression levels of desmin, TNF-α, NFκB p65, and NOX-1 mRNA in renal cortical tissues of 15-week-old experimental animals. Values are expressed as means ± s.e.m. Expression levels of all four genes were increased in LZR-HFD animals when compared with LZR-RD animals, and were also increased in OZR-HFD animals when compared with OZR-RD animals. TEMPOL treatment attenuated these increases in both LZR and OZR animals. (**b**) NFκB p65 DNA binding activity in renal cortical nuclear extracts of experimental animals as determined by electrophoretic mobility shift assay. Densitometry values are expressed as means ± s.e.m. HFD increased NFκB p65 DNA binding activity in both LZR and OZR; TEMPOL treatment attenuated these increases. $^{*}P < 0.05$ vs. LZR-RD, $^{\#}P < 0.05$ vs. LZR-

HFD, $^{@}P < 0.05$ vs. LZR-HFD-TEM, $^{\$}P < 0.05$ vs. OZR-RD, $^{\dagger}P < 0.05$ vs. OZR-HFD, $^{\ddagger}P < 0.05$ vs. OZR-HFD-TEM. HFD, high-fat diet; LZR, lean Zucker rat; NFκB, nuclear factor κB; NOX-1, NAD(P)H oxidase-1; OZR, obese Zucker rat; RD, regular diet; TEMPOL, superoxide scavenger 4-hydroxy-2,2,6,6-tetramethylpiperidinyloxy; TNF-α, tumor necrosis factor-α.

Table 1

Food intakes, body and organ weights, and blood pressures of rat groups

Parameters	LZR-RD	LZR-HFD	LZR-HFD-TEMPOL	OZR-RD	OZR-HFD	OZR-HFD-TEMPOL
Food intake (g)	24.6 ± 0.54 **	21.75 ± 0.93 *	18.5 ± 2.25	22.5 ± 1.9 ††	19.4 ± 0.75 †,†††	20.0 ± 0.05 ††
Body weight (g)	382 ± 4.75 **	409.6 ± 2.4 *	407.5 ± 4.3	542.8 ± 1.91	617.8 ± 4.6	613.2 ± 4.4
Weight gain (g)	186 ± 11 **	284 ± 4.3 *,***	227.60 ± 3.0 **	368 ± 10 ††	436.80 ± 8.8 †,†††	386.40 ± 7.9 ††
Heart (g)	0.90 ± 0.003	1.06 ± 0.001	1.14 ± 0.02	1.17 ± 0.01	1.20 ± 0.03	1.16 ± 0.01
Kidney (g)	1.2 ± 0.002	1.26 ± 0.05	1.25 ± 0.03	1.34 ± 0.08	1.71 ± 0.02	1.58 ± 0.04
Liver (g)	11.50 ± 0.17	13.09 ± 0.71	12.64 ± 0.36	17.38 ± 0.78 ††	24.65 ± 0.65 †,†††	22.5 ± 0.61
Abdominal fat (g)	3.24 ± 0.3 **	14.61 ± 0.94 *,***	6.66 ± 0.49 **	19.86 ± 0.35 †,†††	35.67 ± 1.24 †,†††	31.43 ± 1.22 ††
MAP (mm Hg)	102 ± 3 †,††,†††	103 ± 4 †,††,†††	100 ± 2 †,††,†††	127 ± 6 *,**,***,†††	129 ± 4 *,**,***,†††	109 ± 5 *,**,***,†,††
SBP (mm Hg)	121 ± 3 †,††,†††	124 ± 3 †,††,†††	118 ± 4 †,††,†††	141 ± 5 *,**,***,†††,†††	157 ± 6 *,**,***,†,†††	135 ± 4 *,**,***,††

The parameters of 15-week-old rats were compared. Values are expressed as means ± s.e.m. Statistical analyses were performed using one-way ANOVA or one-way ANOVA with repeated measurements followed by a post hoc Bonferroni test. $P \leq 0.05$ was considered significant.

HFD, high-fat diet; LZR, lean Zucker rat; MAP, mean arterial blood pressure; OZR, obese Zucker rat; RD, regular diet; SBP, systolic blood pressure; TEMPOL, superoxide scavenger 4-hydroxy-2,2,6,6-tetramethylpiperidinyloxy.

*
$P < 0.05$ vs. LZR-RD,

**
$P < 0.05$ vs. LZR-HFD,

***
$P < 0.05$ vs. LZR-HFD-TEM,

†
$P < 0.05$ vs. OZR-RD,

††
$P < 0.05$ vs. OZR-HFD,

†††
$P < 0.05$ vs. OZR-HFD-TEM.

Table 2

Metabolic characteristics of lean and OZRs at study end

Parameters	LZR-RD	LZR-HFD	LZR-HFD-TEMPOL	OZR-RD	OZR-HFD	OZR-HFD-TEMPOL
Glucose (mg/dl)	172 ± 19.5 **	215 ± 3.75 *,***	189.9 ± 71.8 **	193.60 ± 6.78 ††	307.8 ± 6.30 †,†††	269.5 ± 7.2 ††
BUN (mg/dl)	18.5 ± 0.25 **	28 ± 0.4 *,***	15.50 ± 0.56 **	19.20 ± 0.59 ††	50.0 ± 0.80 †,†††	18.4 ± 0.42 ††
Creatinine (mg/dl)	0.49 ± 0.005 **	0.7 ± 0.02 *,***	0.43 ± 0.01 **	0.56 ± 0.01 ††	1.04 ± 0.02 †,†††	0.6 ± 0.01 ††
BUN/creatinine (mg/mg)	37.75 ± 2.5	40 ± 2.1	36.04 ± 0.18	35.0 ± 1.44 ††	48.28 ± 0.60 †,†††	28.1 ± 0.41 ††
CRP (ng/ml)	31.20 ± 0.97 **	82.34 ± 2.85 *,***	55.80 ± 0.27 **	57.48 ± 1.69 ††	93.17 ± 1.59 †,†††	53.08 ± 0.72 ††
Insulin (ng/ml)	1.92 ± 0.01 **	10.04 ± 0.23 *,***	6.9 ± 0.17 **	20.28 ± 1.69 ††	92.28 ± 2.76 †,†††	24.85 ± 2.13 ††
Urinary albumin excretion (mg/dl)	10.83 ± 0.17 **	34.55 ± 0.76 *,***	15.32 ± 0.49 **	54.14 ± 1.82 ††	117.79 ± 1.22 †,†††	71.14 ± 3.32 ††

The parameters of 15-week-old rats were compared. Values are expressed as means ± s.e.m. Statistical analyses were performed using one-way ANOVA followed by a post hoc Bonferroni test. $P \leq 0.05$ was considered significant.

BUN, blood urea nitrogen; CRP, C-reactive protein; HFD, high-fat diet; LZR, lean Zucker rat; OZR, obese Zucker rat; RD, regular diet; TEMPOL, superoxide scavenger 4-hydroxy-2,2,6,6-tetramethylpiperidinyloxy.

*
$P < 0.05$ vs. LZR-RD,

**
$P < 0.05$ vs. LZR-HFD,

***
$P < 0.05$ vs. LZR-HFD-TEM,

†
$P < 0.05$ vs. OZR-RD,

††
$P < 0.05$ vs. OZR-HFD,

†††
$P < 0.05$ vs. OZR-HFD-TEM.

Table 3

Lipid profiles of lean and OZRs at study end

Parameters	LZR-RD	LZR-HFD	LZR-HFD-TEMPOL	OZR-RD	OZR-HFD	OZR-HFD-TEMPOL
Triglycerides (mmol/l)	1.41 ± 0.02 **	2.12 ± 0.06 *,***	0.72 ± 0.01 **	2.42 ± 0.06 ††	9.10 ± 0.28 †,†††	2.70 ± 0.32 ††
Cholesterol (mmol/l)	0.52 ± 0.04 **	0.99 ± 0.03 *,***	0.78 ± 0.03 **	1.62 ± 0.08 ††	4.0 ± 0.15 †,†††	2.19 ± 0.06 ††
HDL–c (mmol/l)	0.28 ± 0.007 **	0.16 ± 0.01 *,***	0.36 ± 0.009 **	0.42 ± 0.018 ††	0.26 ± 0.006 †,†††	1.14 ± 0.02 ††
VLDL–c (mmol/l)	0.13 ± 0.01 **	0.18 ± 0.004 *,***	0.07 ± 0.005 **	0.19 ± 0.002 ††	0.32 ± 0.008 †,†††	0.18 ± 0.02 ††

The parameters of 15-week-old rats were compared. Values are expressed as means $\pm$ s.e.m. Statistical analyses were performed using one-way ANOVA followed by a post hoc Bonferroni test. $P \leq 0.05$ was considered significant.

HDL–c, high-density lipoprotein-cholesterol; HFD, high-fat diet; LZR, lean Zucker rat; OZR, obese Zucker rat; RD, regular diet; TEMPOL, superoxide scavenger 4-hydroxy-2,2,6,6-tetramethylpiperidinyloxy; VLDL, very low-density lipoprotein-cholesterol.

*
$P < 0.05$ vs. LZR-RD,

**
$P < 0.05$ vs. LZR-HFD,

***
$P < 0.05$ vs. LZR-HFD-TEM,

†
$P < 0.05$ vs. OZR-RD,

††
$P < 0.05$ vs. OZR-HFD,

†††
$P < 0.05$ vs. OZR-HFD-TEM.

Table 4

Glomerular morphological findings from lean and OZRs from each experimental group

Parameter	LZR-RD	LZR-HFD	LZR-HFD-TEM	OZR-RD	OZR-HFD	OZR-HFD-TEM
Glomerular diameter (μm)	8.32 ± 0.08 **	7.45 ± 0.02 *, ***	8.62 ± 0.22 **	8.93 ± 0.01 ††	10.68 ± 0.67 †,†††	8.77 ± 0.06 ††
Glomerular area (μm²)	55.96 ± 0.62 **	45.01 ± 0.28 *, ***	60.71 ± 3.83 **	64.60 ± 0.01 ††	70.30 ± 1.95 †,†††	63.66 ± 1.41 ††
Glomerular circumference (μm)	26.21 ± 0.25	24.73 ± 0.98	27.13 ± 0.73	28.09 ± 0.00	37.45 ± 4.94	27.72 ± 0.29

The parameters of 15-week-old rats were compared. Values are expressed as means ± s.e.m. Statistical analyses were performed using one-way ANOVA followed by a post hoc Bonferroni test. $P \leq 0.05$ was considered significant.

LZR, lean Zucker rat; OZR, obese Zucker rat; RD, regular diet; TEMPOL, superoxide scavenger 4-hydroxy-2,2,6,6-tetramethylpiperidinyloxy.

*
$P < 0.05$ vs. LZR-RD,

**
$P < 0.05$ vs. LZR-HFD,

***
$P < 0.05$ vs. LZR-HFD-TEM,

†
$P < 0.05$ vs. OZR-RD,

††
$P < 0.05$ vs. OZR-HFD,

†††
$P < 0.05$ vs. OZR-HFD-TEM.